Biodegradation of saturate fraction of crude oil and production of signature carboxylic acids

Kevin Iyere Ehiosun, Simon Godin, Vicmary Vargas, Hugues Preud'Homme, Regis. Grimaud, Ryszard Lobinski

Biodegradation of saturate fraction of crude oil and production of signature carboxylic acids

Kevin Iyere Ehiosun [a,b,1,*], Simon Godin [a], Vicmary Vargas [a], Hugues Preud'homme [a], Régis Grimaud [a], Ryszard Lobinski [a]

[a] *Université de Pau et des Pays de l'Adour, E2S UPPA, CNRS, IPREM, Pau, France.*

[b] *Department of Biochemistry, Edo State University Uzairue, Edo State, Nigeria.*

** Corresponding author. Université Paris-Saclay, INRAE, PRocédés biOtechnologiques au Service de l'Environnement, 92761, Antony, France.*

E-mail address: kiehiosun@univ-pau.fr

[1] Present address: Université Paris-Saclay, INRAE, PRocédés biOtechnologiques au Service de l'Environnement, 92761, Antony, France.

Abstract

Bacteria degrading large portion of saturated hydrocarbons are important for crude oil bioremediation. This study investigates *Novosphingobium* sp. S1, *Gordonia amicalis* S2 and *Gordonia terrae* S5 capability of degrading wide range of saturated hydrocarbons from Congo Bilondo crude oil and discusses the degradation pathway. A parallel analytical approach combining GC-MS and LC-HRMS enabled characterization of saturated hydrocarbons and comprehensive determination of carboxylic acid metabolites produced during biodegradation, respectively. Results showed that the three strains could efficiently degrade the *n*-alkanes (C_{10}-C_{28}) as well as methyl-substituted alkanes (C_{11}-C_{26}). The series of mono-, hydroxy- and dicarboxylic acids identified in this study confirmed the active biodegradation of the saturate fraction and suggest their degradation was via the bi-terminal oxidation pathway. This is the first study linking these bacterial species to bi-terminal oxidation of the saturated hydrocarbons. The study highlights the potential application of the bacterial strains in the bioremediation of crude oil contaminated sites. Additionally, while carboxylic acids is indicated as a suitable and valuable metabolic biomarker, its application is considered feasible and cost effective for rapid monitoring and evaluation of hydrocarbon biodegradation.

Keywords: crude oil, hydrocarbon, carboxylic acid, SARA, saturate fraction, *Gordonia*, *Novosphingobium*

1. Introduction

Crude oil is projected to remain a global source of revenue, energy and feedstock for industries (Speight, 2017). However, crude oil is also considered a major source of hydrocarbon pollution (Coronel Vargas et al., 2020; Khan et al., 2018). Saturated hydrocarbons represent the highest portion of most crude oil types with an estimated abundance of 20-50% (Cappelletti et al., 2019; Varjani, 2017). Saturated hydrocarbons carbon chains can be aliphatic (*n*-alkanes), branched (iso-alkanes and acyclic isoprenoids) or cyclic (cyclo-alkanes and cyclic isoprenoids) containing one or more saturated rings.

Microbial degradation is an effective strategy used in bioremediation of crude oil pollution because microorganisms, such as bacteria, can degrade hydrocarbons to carbon dioxide and water (Das, 2014). Saturated hydrocarbons are characterized by low chemical reactivity and poor water solubility, which effectively limit availability and accessibility to the degrading microorganisms (Singh et al., 2012). Although low molecular weight saturated hydrocarbons are sparingly available to the degrading microbe, they are very toxic. The high molecular weight saturates are insoluble in aqueous medium. Nonetheless, they are degraded by a (bio)surfactant- or biofilm-mediated process that facilitates pseudo-solubilisation and assimilation of hydrocarbons (Dasgupta et al., 2013; Ehiosun et al., 2022a; Karlapudi et al., 2018; Sivadon et al., 2019). Few bacteria are known to degrade a wide spectrum of saturated hydrocarbons (Chen et al., 2017; Liu et al., 2020; Tanzadeh et al., 2020). This makes characterization of bacteria able to degrade large fraction of saturated hydrocarbons essential for bioremediation.

Aerobic biodegradation of saturated hydrocarbons involves terminal and/or sub-terminal oxidation that produces alcohols, which are converted into carboxylic acids (Singh et al., 2012). Occasionally, the produced monocarboxylic acids can further be oxidized through ω-hydroxylation before conversion into dicarboxylic acids (Ji et al., 2013). The production of

carboxylic acids during hydrocarbon biodegradation was reported as a viable indicator for biodegradation (Ehiosun et al., 2022b; Gruner et al., 2017; Watson et al., 2002). Carboxylic acids are also indicative of the mechanisms or metabolic pathways adopted by the degrading bacteria. However, elucidation of metabolic pathways by studying the metabolites produced requires the development of dedicated analytical protocols.

An analytical study of both the residual hydrocarbons and the produced carboxylic acids during biodegradation are useful for understanding and evaluating the degradation process. Gas chromatography (GC) and liquid chromatography (LC) coupled to high-resolution accurate-mass (HRAM) mass spectrometry (MS) remain the principal tools to characterize hydrocarbon biodegradation (Imam et al., 2019). Although GC-MS is a more common technique for analysing hydrocarbon biodegradation (Prince and Walters, 2022), it is not amenable to the analysis of the produced carboxylic acids, which are polar or non-volatile, without a cumbersome derivatization step. LC-MS provides an easy, direct, rapid, robust, and quantitative method of detection of the produced carboxylic acids without prior derivatization (Godin et al., 2020). Nevertheless, residual hydrocarbon analysis is generally preferred through GC because of the non-polar and thermally stable properties of hydrocarbons.

Thus, the objectives of this study were 1) to investigate the capability of alkane-degrading bacterial strains to degrade the saturate fraction of Congo Bilondo crude oil, 2) to develop and apply a parallel analytical methodology that combines the efficiency of GC-MS with LC-HRMS for saturated hydrocarbons and produced carboxylic acids characterization during biodegradation and 3) to evaluate the suitability of carboxylic acids as valuable metabolic biomarker for monitoring hydrocarbon biodegradation.

2. Materials and methods

2.1 Alkane-degrading bacteria

Novosphingobium sp. S1, *Gordonia amicalis* S2 and *Gordonia terrae* S5, used within this study were described elsewhere (Ehiosun et al., 2022a).

2.2 Biodegradation of the saturate fraction of Congo Bilondo crude oil

2.2.1 Fractionation of Congo Bilondo crude oil

n-Heptane was use to fractionate Congo Bilondo crude oil into maltene and asphaltene based on the American Society for Testing and Materials (ASTM) D4124-09 standard procedure (ASTM, 2018). Briefly, the crude oil (85.2 g) was dissolved in *n*-heptane (1:40, w/v) to induce precipitation of asphaltene for 72 h. Afterwards, this mixture was filtered using Whatman® filter paper, Grade 1 placed in a Büchner funnel. Asphaltene was retained on the filter paper and was recovered after air-drying the filter paper at room temperature. The filtrate was recovered as maltene and was concentrated by rotary evaporation at 70 °C and 90 rpm.

Thereafter, 10 g of the maltene was fractionated using column chromatography. For this, a glass column (32.5 cm length and 3.5 cm internal diameter) was used. The stationary phase was a bed of silica gel with a pore volume of 0.75 cm^3 g^{-1}. The saturate, aromatic and resin fractions were obtained by eluting the column with *n*-hexane, toluene, and chloroform/methanol (9:1, v/v), respectively.

2.2.2 Characterization of saturate fraction of Congo Bilondo crude oil by GC-MS

One microlitre of the saturate fraction was injected, in splitless mode, into the GC-MS instrument (Thermo Scientific™ TRACE™ 1300 Series– ISQ QD300 GCMS System, ThermoFisher Scientific, Illkirch-Graffenstaden, France). The GC-MS instrument was fitted with a Phenomenex® Zebron™ ZB-624_{PLUS}™ column with dimension 30 m × 0.25 mm × 1.40 µm.

Using helium gas at a flow rate of 1.5 mL min^{-1}, oven temperature was initially kept at 50 °C for a minute. After, it was raised to 150 °C at 20 °C min^{-1} and afterward to 250 °C at 10 °C min^{-1}. Finally, the temperature was ramped up by 15 °C min^{-1} to 300 °C and kept for 5.6 min. Automation and data processing were done on Thermo Scientific™ Chromeleon™ 6.8 Chromatography Data System (CDS) with an embedded National Institute of Standards and Technology (NIST) 2017 database.

2.2.3 Biodegradation of saturate fraction

Incomplete Mineral Medium was used for biodegradation study (Ehiosun et al., 2022a). The saturate fraction (0.1%, v/v) was added to 5 mL of the medium without bacteria (abiotic control) and with bacteria in triplicate. The cultures were incubated at 30 °C and 50 rpm in an orbital shaker incubator. The experiments were stopped on day 0, 3, and 5 for assessment of residual hydrocarbons and extracellular metabolites.

2.2.4 Extraction of extracellular metabolites in culture

Supernatants devoid of bacterial cells were obtained from each culture (abiotic and biotic) through centrifugation and filtration for extracellular metabolite screening as described earlier (Ehiosun et al., 2022a). Pending LC-MS analysis, the recovered supernatants were preserved at -20 °C.

2.3 Analysis for residual hydrocarbons and identification of extracellular metabolites

2.3.1 Residual saturated hydrocarbons analysis by GC-MS

Hydrocarbons remaining in culture were extracted using 5 mL *n*-hexane spiked with 0.1% deuterated dodecane. This mixture was vigorously shaken for 20 min at 400 oscillation min^{-1} for optimum extraction of the residual hydrocarbons. Thereafter, samples were kept at -20 °C for 3 h to recover only the organic phase. GC-MS conditions and data analysis discussed in Section 2.2.2 were used to analyse the residual hydrocarbons.

142 *2.3.2 Evaluating biodegradation efficiency*

143 *n*-Alkanes (C_{10}-C_{24}) present in the saturate fraction were determined using a calibration curve of
144 standard *n*-alkanes mix (C_{10}-C_{24}). The measured concentration was used to calculate the
145 biodegradation efficiency against those of abiotic controls using the equation below.

146 $$\text{Biodegradation efficiency (\%)} = \frac{CA - CB}{CA} \times 100 \quad (1)$$

147 Where CA and CB are the concentration of the *n*-alkanes (C_{10}-C_{24}) in abiotic control and bacteria
148 treated samples, respectively.

149 Biodegradation efficiency of the other hydrocarbons without standards was estimated using their
150 response ratio (*R*), defined by equation 2:

151 $$\text{Response ratio (R)} = \frac{PS}{PI} \quad (2)$$

152 PS is the peak area of each compound in the saturate fraction; and PI represents peak area of 0.1%
153 deuterated dodecane (internal standard).

154 Subsequently, the estimated R was used to calculate the biodegradation efficiency using the
155 equation below:

156 $$\text{Biodegradation efficiency (\%)} = \frac{RA - RB}{RA} \times 100 \quad (3)$$

157 RA and RB are the response ratio (R) in an abiotic control and bacteria treated samples,
158 respectively.

159 *2.3.3 Profiling carboxylic acid metabolites by LC-MS/MS*

160 LC-HRMS instrumentation and methodology previously described by Ehiosun *et al* (Ehiosun et
161 al., 2022a) were used to screen for extracellular metabolites in aliquots of the recovered
162 supernatants during biodegradation of the saturate fraction. Similarly, acquired LC-HRMS data

was processed with the ThermoFisher Scientific™ Compound Discoverer 2.1™ application associated with Chemspider and mzCloud databases.

2.3.4 Structural elucidation of carboxylic acid metabolites by LC-MS^3

The same chromatographic system and conditions in section 2.3.3 were applied to targeted analysis using the ThermoFisher Scientific™ Orbitrap Fusion™ Lumos™ Tribrid™ mass spectrometer. Collision-induced dissociation (CID) was employed for fragmentation at collision energies ramping from CID15 to CID45 in full MS scan modes.

3. Results and discussion

3.1 fractional composition of Congo Bilondo crude oil

Fractionation of Congo Bilondo crude oil into saturate, aromatic, resin and asphaltene (SARA) fractions was done before biodegradation study. This permitted the study of the saturate fraction without interference of the other fractions. SARA fractionation produces saturate and aromatic hydrocarbons, resins, and asphaltenes subject to their solubility, polarity and adsorption (Shishkova et al., 2022). The result from the SARA fractionation is presented in Table 1. Firstly, asphaltene was precipitated using *n*-heptane because of its insolubility in low molecular weight alkanes (Branthaver and Huang, 2015). After this process, 0.3% of asphaltene and 99.6% of maltene by weight were recovered. The low amount of asphaltene indicates that the crude oil is a paraffinic crude oil. Subsequent fractionation of the maltene (10 g) produced saturates (50.4 ± 1.7%), aromatics (32.8 ± 1.3%) and resins (14.4 ± 0.8%) by weight with 97.6 ± 1.4% recovery of the total mass initially added.

The saturate fraction was a less viscous yellow-green liquid as shown in Figure S1 (supplementary material). The aromatic fraction was brownish and more viscous

while resin was the most viscous with a dark brown colour. The asphaltene fraction was a black dry flake. Similar physical characteristics were reported elsewhere (Gaspar et al., 2012).

4.3.2 Characterization of the saturate fraction by GC-MS

Figure S2 shows the GC-MS chromatogram of the saturate fraction. Hydrocarbons detected in the saturate fraction included *n*-alkanes (C_{10}-C_{28}) and various monomethyl-, dimethyl, trimethyl-, and tetramethyl-substituted alkanes (isoprenoids). These hydrocarbons were annotated based on their characteristic fragments at m/z 43, 57, 71 and 85 (Figure S3) and matched with standards and the NIST 2017 database. The short chain alkanes ($\leq C_9$) were not detected in the fraction probably due to losses during SARA fractionation. The risk of losing the more volatile hydrocarbons is one limitation of SARA fractionation (Kharrat et al., 2007; Rezaee et al., 2020). *n*-Hexadecane was observed as the most abundant among the detected hydrocarbons with a concentration of 337 ± 68 µg L^{-1} (Table 2). *n*-Hexadecane is an abundant alkane found in crude oil (Domdi et al., 2021; Meng et al., 2017) and it is a common model hydrocarbon for biodegradation studies of long-chain alkanes. Pristane and phytane were observed as the dominant isoprenoids (Jovančićević et al., 2008). Some hydrocarbons were not resolved and identified probably due to problem of instrumental sensitivity, ionization, or database match (Farmani and Schrader, 2019).

3.3 Biodegradation of the saturate fraction

Figure 1 shows the GC-MS chromatograms obtained on day 3 and 5 of the biodegradation study. They indicate that the profile of the saturate fraction changed significantly in comparison with the abiotic control, at different extent as a function of the bacteria strain. An important observation is that the three bacterial strains can efficiently use the *n*-alkanes (C_{10}-C_{28}) as well as the methyl-substituted alkanes (C_{11}-C_{26}) for growth and energy. Remarkably, this illustrate that these strains can effectively metabolize a broad spectrum of the saturated hydrocarbons and highlights their

bioremediation potential. Additionally, these strains grew at the oil-water interface by forming biofilms. Biofilm formation was reported to effectively reduce the distance for the mass transfer and assimilation of hydrocarbons (Abbasnezhad et al., 2011). Moreover, cells and secreted degradation factors were reported to be localized within the biofilm matrix for effective degradation (Ennouri et al., 2017; Sivadon et al., 2019).

The biodegradation efficiency of each saturated hydrocarbon for the bacterial strains is shown in Table 3. The medium-chain *n*-alkanes (C_{10}-C_{19}) were efficiently degraded by the strains, with degradation rates above 70% on day 5. Most odd-number carbon *n*-alkanes (C_{15}-C_{19}) were completely degraded. This could be attributed to the loose configuration of odd-number carbon atoms compared to even-carbon-number *n*-alkanes that are more symmetrical (Liu et al., 2020). However, degradation rates of long-chain alkanes (C_{20}-C_{28}) were relatively lower with *G. terrae* S5 than with the other two strains. *Gordonia* strains are known to degrade C_8-C_{36} alkanes (Kim et al., 2019; Mikolasch et al., 2015). Interestingly, *Novosphingobium* sp. S1 showed a high capability degrading the saturated hydrocarbons even though this genus is known to degrading aromatic hydrocarbons (Kertesz and Kawasaki, 2010).

The methyl-substituted alkanes were efficiently degraded by the three strains. For instance, 2,3,7 trimethyloctane, 2,6,10-trimethyltridecane and 2,6,10-trimethylpentadecane were completely degraded on day 5. Although pristane and phytane are considered relatively resistant to biodegradation due to being highly branched, they were degraded with degradation efficiency reaching 87 ± 7 and 100%, respectively, on day 5 for *Novosphingobium* sp. S1. Equally, biodegradation efficiencies of pristane and phytane were 91 ± 4 and 98 ± 2%, respectively, within 5 d for *G. amicalis* S2 but were 77 ± 5 and 62 ± 7% for *G. terrae* S5. Evidently, the biodegradation of *n*-alkanes and isoprenoids occur at approximately the same rate. Similarly, a near complete degradation of phytane and pristane after 20 d was reported using a bacterial

consortium (Bidja Abena et al., 2020). In contrast, pristane and phytane remained detected within 90 d of biodegradation in another study (Liu et al., 2020). Pristane and phytane are degraded mainly via mono-, di-terminal and sub-terminal oxidation with an initial activation by hydroxylation (Abbasian et al., 2015).

3.4 Identification of carboxylic acids metabolites and elucidation of degradation pathway

The separation efficiency of carboxylic acids in the culture medium and their ionization conditions were optimized before LC-HRMS analysis. The LC-HRMS methodology was validated by analysing these three carboxylic acid standards; hexadecanoic acid, 16-hydroxyhexadecanoic acid and benzoic acid (Figure S4). A good separation efficiency and sensitivity was observed with the standards. However, hexadecanoic acid was identified as a carry-over contaminant. Therefore, hexadecanoic acid was excluded during screening and selection of metabolites. Furthermore, the acquired data sets (m/z, retention times, intensities etc.) were large and complex. Overcoming this challenge during data processing necessitated developing targeted workflows. Consequently, to focus on compounds of interest that are specific to the biodegradation process, the area ratio of compounds over time, that indicates when they appear and disappeared, was used. In addition, compounds in blanks, abiotic control, and at the start of experiment (day 0) were disregarded. Likewise, compounds that were not found in replicates were omitted. Finally, molecular formulas were determined based on the ratio of carbon to hydrogen atoms, fragmentation pattern and database match (Chemspider and mzCloud).

Fourteen carboxylic acids identified as extracellular metabolites during degradation of the saturate fraction by the three bacterial strains are presented in Table 4. The carboxylic acids ranged from C_{10}-C_{20} and comprised of monocarboxylic acids, hydroxylated carboxylic acids, and dicarboxylic acids. While most of the carboxylic acids were identified by database search, a fragmentation pattern characteristic of dehydration, decarboxylation and dealkylation was observed for all the

258 compounds (Table S1). However, short chain fragments were not obtained in MS^2 nor MS^3, as an
259 increase in the fragmentation energy beyond CID45 resulted in the loss of the precursor.

The appearance of C_{10}-C_{20} straight chain carboxylic acids implies degradation of specific C_{10}-C_{20} alkanes as illustrated in Table 4. For instance, undecanoic acid is produced from undecane while tetradecanoic, 14-tetradecanoic and tetradecanedioic acid are degradation products of tetradecane. Bacteria are known to degrade alkanes through mono-terminal, bi-terminal or sub-terminal pathways, with the first found to be ubiquitous (Varjani, 2017). These pathways are catalyzed by oxygenases like cytochrome CYP153A enzymes and alkane hydroxylases (Ji et al., 2013). However, the series of mono-, hydroxy- and dicarboxylic acids found in this study suggested that their production was via the bi-terminal oxidation or dicarboxylic acid pathway. Alkane-activating monooxygenases produce oxygen radicals to circumvent alkanes' poor reactivity (Singh et al., 2012). After the formation of the initial terminal oxidation products (primary alcohol and aldehyde), without breaking of the carbon chain, the degradative pathway branches into bi-terminal oxidation (Figure 2). The *ω*-hydroxylation of monocarboxylic acids produces *ω*-hydroxycarboxylic acids that are transformed into dicarboxylic acids, and later channelled into the β-oxidation pathway (Ji et al., 2013). Most likely, this is a first report linking these bacterial species to a bi-terminal oxidation of alkanes. Hydroxylated fatty acids production was reported for bacterial strains degrading *n*-hexadecane (Rodrigues et al., 2020) and many dicarboxylic acids were observed during degradation of *n*-octacosane (Oberding and Gieg, 2018). The results supports carboxylic acids as useful indicators for tracing microbial activities during hydrocarbon biodegradation. Characterization of metabolic biomarkers, such as carboxylics, are useful in the design and evaluation of bioremediation strategies (Oka et al., 2011).

Although the presence of the carboxylic acids indicates active degradation of hydrocarbons, why they are present in the extracellular medium remains unclear. Nonetheless, the extracellular oxidation of *n*-hexadecane was reported before (Meng et al., 2017). Furthermore, the strains used in this study form biofilm in the presence of hydrocarbons (Ehiosun et al., 2022a). Thus, we can speculate that hydroxylation and the subsequent oxidations of alkanes occurs within the

285 extracellular matrix of the biofilm. Notably, the extracellular matrix of biofilm was described as
286 an external digestive system favouring hydrocarbon solubilisation, digestion and assimilation
287 (Sivadon et al., 2019). These metabolites could also originate from leakage of cells by active or
288 passive excretion and/or through cell lysis and death (Heyen et al., 2021). Figure 3 shows the
289 production of carboxylic acids for each studied bacterial strain. In one case, 14-
290 hydroxytetradecanoic acid was detected only on day 3 for *G. amicalis* S2 and *Novosphingobium*
291 sp. S1 but was relatively at the same level for *G. terrae* S5 at day 3 and 5. In addition,
292 tetradecanoic acid and 10-propoxydecanoic acid were not detected for *Novosphingobium* sp. S1.

293

294 **4. Conclusion**

295 This study demonstrated the high capability that *Novosphingobium* sp. S1, *Gordonia amicalis* S2
296 and *Gordonia terrae* S5 have with degrading the saturate fraction of Congo Bilondo crude oil. The
297 analytical data obtained from parallel GC-MS and LC-HRMS analyses enabled an in-depth
298 assessment of the biodegradation. While medium-chain and long-chain *n*-alkanes were efficiently
299 degraded by the bacterial strains, most odd-number carbon *n*-alkanes and some methyl-substituted
300 alkanes were completely degraded. The obtained results highlight the potential application of the
301 strains in bioremediation of crude oil polluted sites. Furthermore, the comprehensive
302 determination of the produced carboxylic acids by LC-HRMS was valuable in tracing the
303 biodegradation of specific alkanes. This approach allowed the identification of the bi-terminal
304 oxidation pathway as the most likely metabolic pathway used by the investigated bacterial strains
305 during degradation of the saturate fraction. This underscores carboxylic acids as a suitable and
306 valuable metabolic biomarker for rapid monitoring and evaluation of bioremediation strategies.
307 No doubt, the progressive availability of advanced chromatographic systems coupled to high-

308 resolution mass spectrometry will significantly expand our understanding of the occurring
309 biochemical processes during biodegradation, which is vital for enhanced bioremediation.

310

311

312

313

314

315

316

317

318

319

320

321

322

323

324

325

326

Funding

The authors acknowledge funding from ANR (11-EQPX-0027 MARSS), MesMic E2S-UPPA and ISIFoR-UPPA. Ehiosun was a PTDF PhD scholarship recipient (18/GFC/PHD/024).

346

347

348

349

350

351

352

353

354

355

356

357 **References**

358 Abbasian, F., Lockington, R., Mallavarapu, M., Naidu, R., 2015. A Comprehensive
359 Review of Aliphatic Hydrocarbon Biodegradation by Bacteria. Appl. Biochem.
360 Biotechnol. 176, 670–699. https://doi.org/10.1007/s12010-015-1603-5

361 Abbasnezhad, H., Gray, M., Foght, J.M., 2011. Influence of adhesion on aerobic
362 biodegradation and bioremediation of liquid hydrocarbons. Appl. Microbiol.
363 Biotechnol. 92, 653–675. https://doi.org/10.1007/s00253-011-3589-4

364 ASTM, 2018. Standard Test Method for Separation of Asphalt into Four Fractions.

365 ASTM D4124-09. Annu. B. ASTM Stand. 09, 3–10.
366 https://doi.org/10.1520/D4124-09R18.2

367 Bidja Abena, M., Thérèse, A., Chen, G., Chen, Z., Zheng, X., Li, S., Li, T., Zhong, W.,
368 2020. Microbial diversity changes and enrichment of potential petroleum
369 hydrocarbon degraders in crude oil-, diesel-, and gasoline-contaminated soil. 3
370 Biotech 10, 42. https://doi.org/10.1007/s13205-019-2027-7

371 Branthaver, J.F., Huang, S.C., 2015. Analytical separation methods in asphalt
372 research. Adv. Asph. Mater. Road Pavement Constr. 31–57.
373 https://doi.org/10.1016/B978-0-08-100269-8.00002-7

374 Cappelletti, M., Fedi, S., Zannoni, D., 2019. Degradation of Alkanes in Rhodococcus.
375 Springer, Cham, pp. 137–171. https://doi.org/10.1007/978-3-030-11461-9_6

376 Chen, W., Li, J., Sun, X., Min, J., Hu, X., 2017. High efficiency degradation of alkanes
377 and crude oil by a salt-tolerant bacterium Dietzia species CN-3. Int. Biodeterior.
378 Biodegrad. 118, 110–118. https://doi.org/10.1016/j.ibiod.2017.01.029

379 Coronel Vargas, G., Au, W.W., Izzotti, A., 2020. Public health issues from crude-oil
380 production in the Ecuadorian Amazon territories. Sci. Total Environ. 719, 134647.
381 https://doi.org/10.1016/j.scitotenv.2019.134647

382 Das, S., 2014. Microbial Biodegradation and Bioremediation, Microbial Biodegradation
383 and Bioremediation. Elsevier. https://doi.org/10.1016/C2013-0-13533-7

384 Dasgupta, D., Ghosh, R., Sengupta, T.K., 2013. Biofilm-Mediated Enhanced Crude Oil
385 Degradation by Newly Isolated Pseudomonas Species . ISRN Biotechnol. 2013, 1–

386 13. https://doi.org/10.5402/2013/250749

387 Domdi, L., Lakra, A.K., Mohan, K., Tilwani, Y.M., Jha, N., Arul, V., 2021. Microbial
388 degradation of n-hexadecane using Pseudomonas aeruginosa PU1 isolated from
389 transformer-oil contaminated soil. Biocatal. Agric. Biotechnol. 38, 102213.
390 https://doi.org/10.1016/j.bcab.2021.102213

391 Ehiosun, K.I., Godin, S., Urios, L., Lobinski, R., Grimaud, R., 2022a. Degradation of
392 long-chain alkanes through biofilm formation by bacteria isolated from oil-
393 polluted soil. Int. Biodeterior. Biodegradation 175, 105508.
394 https://doi.org/10.1016/j.ibiod.2022.105508

395 Ehiosun, K.I., Grimaud, R., Lobinski, R., 2022b. Mass spectrometric analysis for
396 carboxylic acids as viable markers of petroleum hydrocarbon biodegradation.
397 Trends Environ. Anal. Chem. 35, e00172.
398 https://doi.org/10.1016/j.teac.2022.e00172

399 Ennouri, H., D'Abzac, P., Hakil, F., Branchu, P., Naïtali, M., Lomenech, A.M., Oueslati,
400 R., Desbrières, J., Sivadon, P., Grimaud, R., 2017. The extracellular matrix of the
401 oleolytic biofilms of Marinobacter hydrocarbonoclasticus comprises cytoplasmic
402 proteins and T2SS effectors that promote growth on hydrocarbons and lipids.
403 Environ. Microbiol. 19, 159–173. https://doi.org/10.1111/1462-2920.13547

404 Farmani, Z., Schrader, W., 2019. A Detailed Look at the Saturate Fractions of
405 Different Crude Oils Using Direct Analysis by Ultrahigh Resolution Mass
406 Spectrometry (UHRMS). Energies 12, 3455. https://doi.org/10.3390/en12183455

Gaspar, A., Zellermann, E., Lababidi, S., Reece, J., Schrader, W., 2012. Characterization of saturates, aromatics, resins, and asphaltenes heavy crude oil fractions by atmospheric pressure laser ionization fourier transform ion cyclotron resonance mass spectrometry. Energy and Fuels 26, 3481–3487. https://doi.org/10.1021/ef3001407

Godin, S., Kubica, P., Ranchou-Peyruse, A., Le Hecho, I., Patriarche, D., Caumette, G., Szpunar, J., Lobinski, R., 2020. An LC-MS/MS Method for a Comprehensive Determination of Metabolites of BTEX Anaerobic Degradation in Bacterial Cultures and Groundwater. Water 12, 1869. https://doi.org/10.3390/w12071869

Gruner, A., Jarling, R., Vieth-Hillebrand, A., Mangelsdorf, K., Janka, C., van der Kraan, G.M., Köhler, T., Morris, B.E.L., Wilkes, H., 2017. Tracing microbial hydrocarbon transformation processes in a high temperature petroleum reservoir using signature metabolites. Org. Geochem. 108, 82–93. https://doi.org/10.1016/j.orggeochem.2017.03.003

Heyen, S., Scholz-Böttcher, B.M., Rabus, R., Wilkes, H., 2021. Release of carboxylic acids into the exometabolome during anaerobic growth of a denitrifying bacterium with single substrates or crude oil. Org. Geochem. 154, 104179. https://doi.org/10.1016/J.ORGGEOCHEM.2020.104179

Imam, A., Suman, S.K., Ghosh, D., Kanaujia, P.K., 2019. Analytical approaches used in monitoring the bioremediation of hydrocarbons in petroleum-contaminated soil and sludge. TrAC - Trends Anal. Chem. 118, 50–64. https://doi.org/10.1016/j.trac.2019.05.023

Ji, Y., Mao, G., Wang, Y., Bartlam, M., 2013. Structural insights into diversity and n-alkane biodegradation mechanisms of alkane hydroxylases. Front. Microbiol. 4. https://doi.org/10.3389/fmicb.2013.00058

Jovančićević, B., Antić, M., Pavlović, I., Vrvić, M., Beškoski, V., Kronimus, A., Schwarzbauer, J., 2008. Transformation of Petroleum Saturated Hydrocarbons during Soil Bioremediation Experiments. Water. Air. Soil Pollut. 190, 299–307. https://doi.org/10.1007/s11270-007-9601-z

Karlapudi, A.P., Venkateswarulu, T.C., Tammineedi, J., Kanumuri, L., Ravuru, B.K., Dirisala, V. ramu, Kodali, V.P., 2018. Role of biosurfactants in bioremediation of oil pollution-a review. Petroleum 4, 241–249. https://doi.org/10.1016/j.petlm.2018.03.007

Kertesz, M.A., Kawasaki, A., 2010. Hydrocarbon-Degrading Sphingomonads: Sphingomonas, Sphingobium, Novosphingobium, and Sphingopyxis, in: Handbook of Hydrocarbon and Lipid Microbiology. Springer Berlin Heidelberg, Berlin, Heidelberg, pp. 1693–1705. https://doi.org/10.1007/978-3-540-77587-4_119

Khan, M.A.I., Biswas, B., Smith, E., Naidu, R., Megharaj, M., 2018. Toxicity assessment of fresh and weathered petroleum hydrocarbons in contaminated soil- a review. Chemosphere 212, 755–767. https://doi.org/10.1016/j.chemosphere.2018.08.094

Kharrat, A.M., Zacharia, J., Cherian, V.J., Anyatonwu, A., 2007. Issues with Comparing SARA Methodologies. Energy & Fuels 21, 3618–3621. https://doi.org/10.1021/ef700393a

Kim, H., Dong, K., Kim, J., Lee, S., 2019. Characteristics of crude oil - degrading bacteria Gordonia iterans isolated from marine coastal in Taean sediment. Microbiologyopen 8, 1–10. https://doi.org/10.1002/mbo3.754

Liu, Y., Wan, Y.Y., Wang, C., Ma, Z., Liu, X., Li, S., 2020. Biodegradation of n-alkanes in crude oil by three identified bacterial strains. Fuel 275, 117897. https://doi.org/10.1016/j.fuel.2020.117897

Meng, L., Li, H., Bao, M., Sun, P., 2017. Metabolic pathway for a new strain Pseudomonas synxantha LSH-7′ : from chemotaxis to uptake of n-hexadecane. Sci. Rep. 7, 39068. https://doi.org/10.1038/srep39068

Mikolasch, A., Omirbekova, A., Schumann, P., Reinhard, A., Sheikhany, H., Berzhanova, R., Mukasheva, T., Schauer, F., 2015. Enrichment of aliphatic, alicyclic and aromatic acids by oil-degrading bacteria isolated from the rhizosphere of plants growing in oil-contaminated soil from Kazakhstan. Appl. Microbiol. Biotechnol. 99, 4071–4084. https://doi.org/10.1007/s00253-014-6320-4

Oberding, L.K., Gieg, L.M., 2018. Methanogenic Paraffin Biodegradation: Alkylsuccinate Synthase Gene Quantification and Dicarboxylic Acid Production. Appl. Environ. Microbiol. 84. https://doi.org/10.1128/AEM.01773-17

Oka, A.R., Phelps, C.D., Zhu, X., Saber, D.L., Young, L.Y., 2011. Dual Biomarkers of Anaerobic Hydrocarbon Degradation in Historically Contaminated Groundwater. Environ. Sci. Technol 45, 3407–3414. https://doi.org/10.1021/es103859t

Prince, R.C., Walters, C.C., 2022. Modern analytical techniques are improving our ability to follow the fate of spilled oil in the environment. Curr. Opin. Chem. Eng. 36, 100787. https://doi.org/10.1016/j.coche.2021.100787

Rezaee, S., Tavakkoli, M., Doherty, R., Vargas, F.M., 2020. A new experimental method for a fast and reliable quantification of saturates, aromatics, resins, and asphaltenes in crude oils. Pet. Sci. Technol. 38, 955–961. https://doi.org/10.1080/10916466.2020.1790598

Rodrigues, E.M., Cesar, D.E., Santos de Oliveira, R., de Paula Siqueira, T., Tótola, M.R., 2020. Hydrocarbonoclastic bacterial species growing on hexadecane: Implications for bioaugmentation in marine ecosystems. Environ. Pollut. 267, 115579. https://doi.org/10.1016/j.envpol.2020.115579

Shishkova, I., Stratiev, D., Venkov Kolev, I., Nenov, S., Nedanovski, D., Atanassov, K., Ivanov, V., Ribagin, S., 2022. Challenges in Petroleum Characterization-A Review. https://doi.org/10.3390/en15207765

Singh, S.., Kumari, B., Mishra, S., 2012. Microbial Degradation of Xenobiotics, Microbial Degradation of Xenobiotics, Environmental Science and Engineering. Springer Berlin Heidelberg, Berlin, Heidelberg. https://doi.org/10.1007/978-3-642-23789-8

Sivadon, P., Barnier, C., Urios, L., Grimaud, R., 2019. Biofilm formation as a microbial strategy to assimilate particulate substrates. Environ. Microbiol. Rep. 11, 749–764. https://doi.org/10.1111/1758-2229.12785

493 Speight, J.G., 2017. Sources and Types of Organic Pollutants, in: Speight, J.G. (Ed.),
494 Environmental Organic Chemistry for Engineers. Elsevier, pp. 153–201.
495 https://doi.org/10.1016/B978-0-12-804492-6.00004-6

496 Tanzadeh, J., Ghasemi, M.F., Anvari, M., Issazadeh, K., 2020. Biological removal of
497 crude oil with the use of native bacterial consortia isolated from the shorelines of
498 the Caspian Sea. Biotechnol. Biotechnol. Equip. 34, 361–374.
499 https://doi.org/10.1080/13102818.2020.1756408

500 Varjani, S.J., 2017. Microbial degradation of petroleum hydrocarbons. Bioresour.
501 Technol. 223, 277–286. https://doi.org/10.1016/j.biortech.2016.10.037

502 Watson, J.S., Jones, D.M., Swannell, R.P.J., Van Duin, A.C.T., 2002. Formation of
503 carboxylic acids during aerobic biodegradation of crude oil and evidence of
504 microbial oxidation of hopanes. Org. Geochem. 33, 1153–1169.
505 https://doi.org/10.1016/S0146-6380(02)00086-4

506

Figures

Figure 1

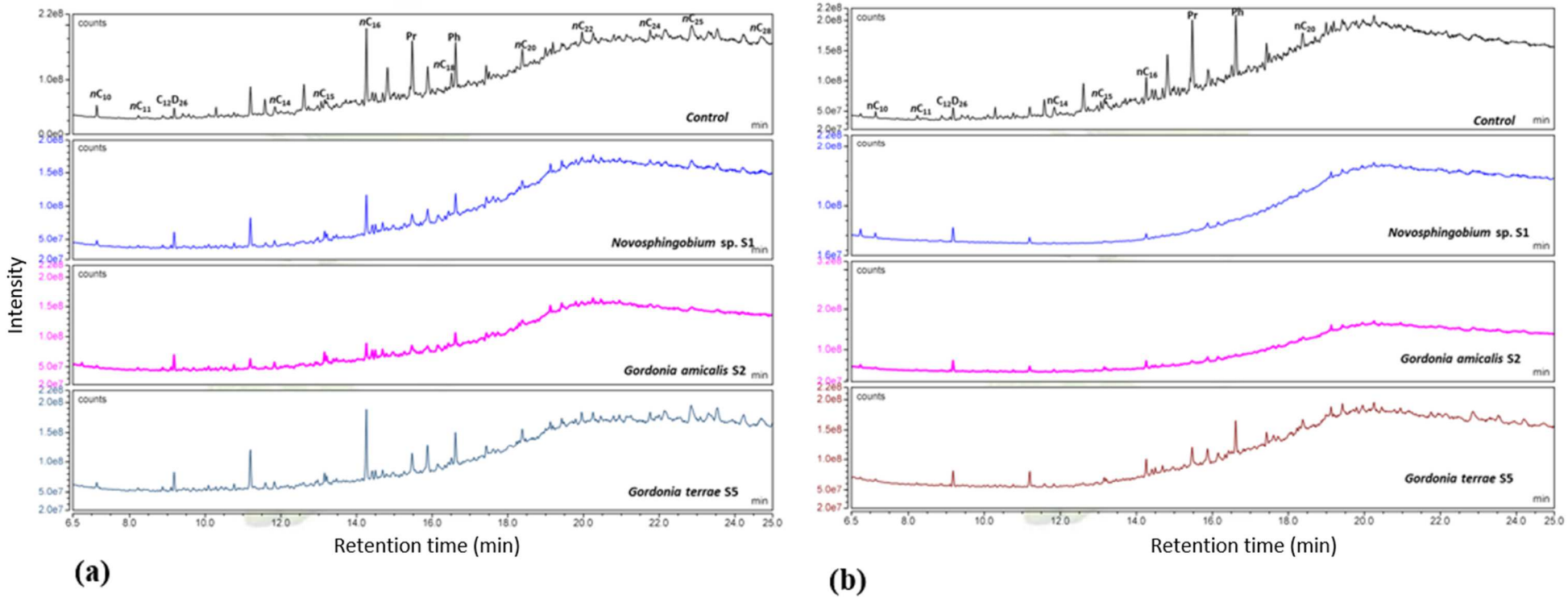

Figure 2

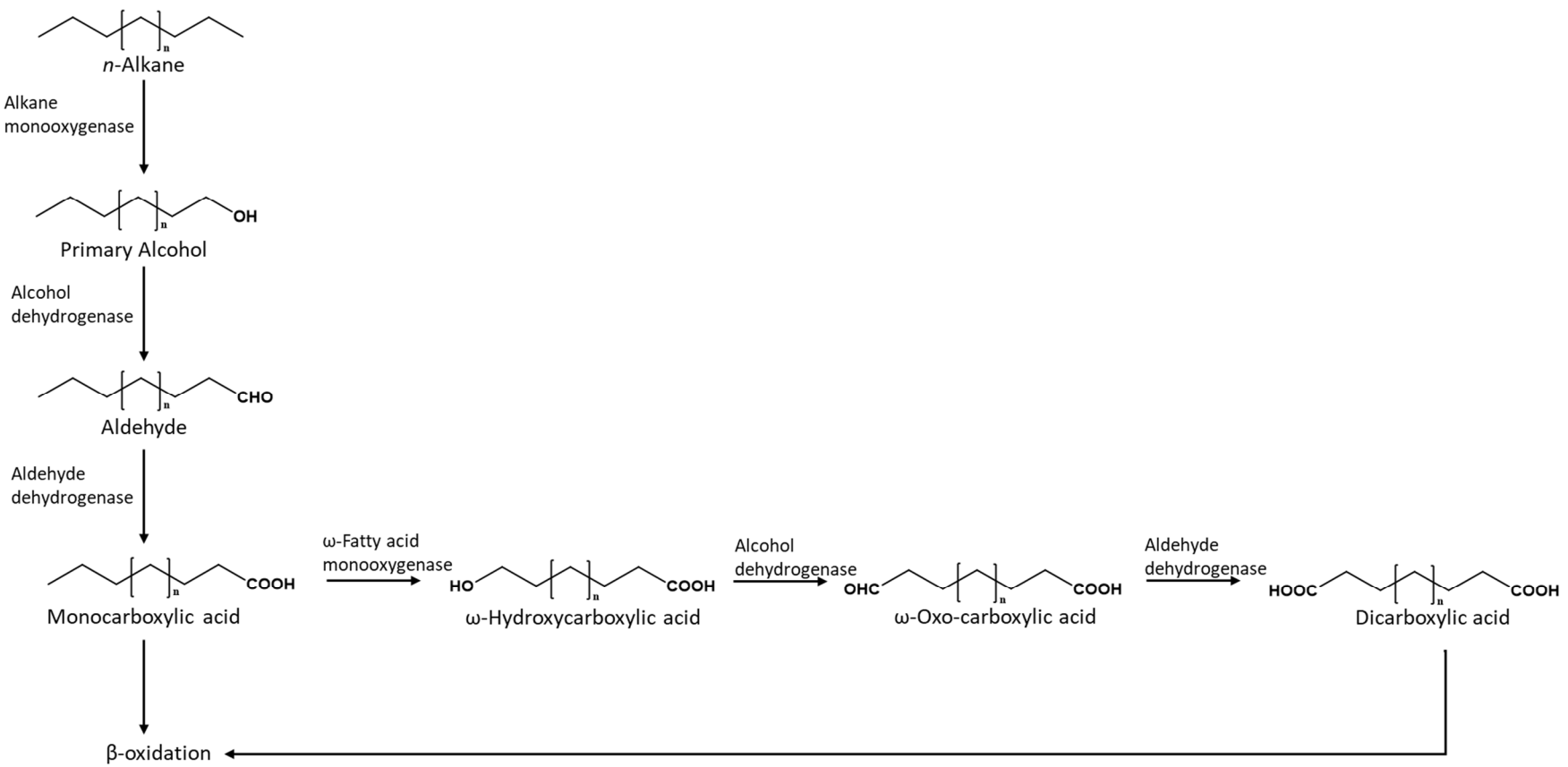
n-Alkane
Alkane monooxygenase
OH
Primary Alcohol
Alcohol dehydrogenase
CHO
Aldehyde
Aldehyde dehydrogenase
COOH
Monocarboxylic acid
ω-Fatty acid monooxygenase
HO
COOH
ω-Hydroxycarboxylic acid
Alcohol dehydrogenase
OHC
COOH
ω-Oxo-carboxylic acid
Aldehyde dehydrogenase
HOOC
COOH
Dicarboxylic acid
β-oxidation

Figure 3

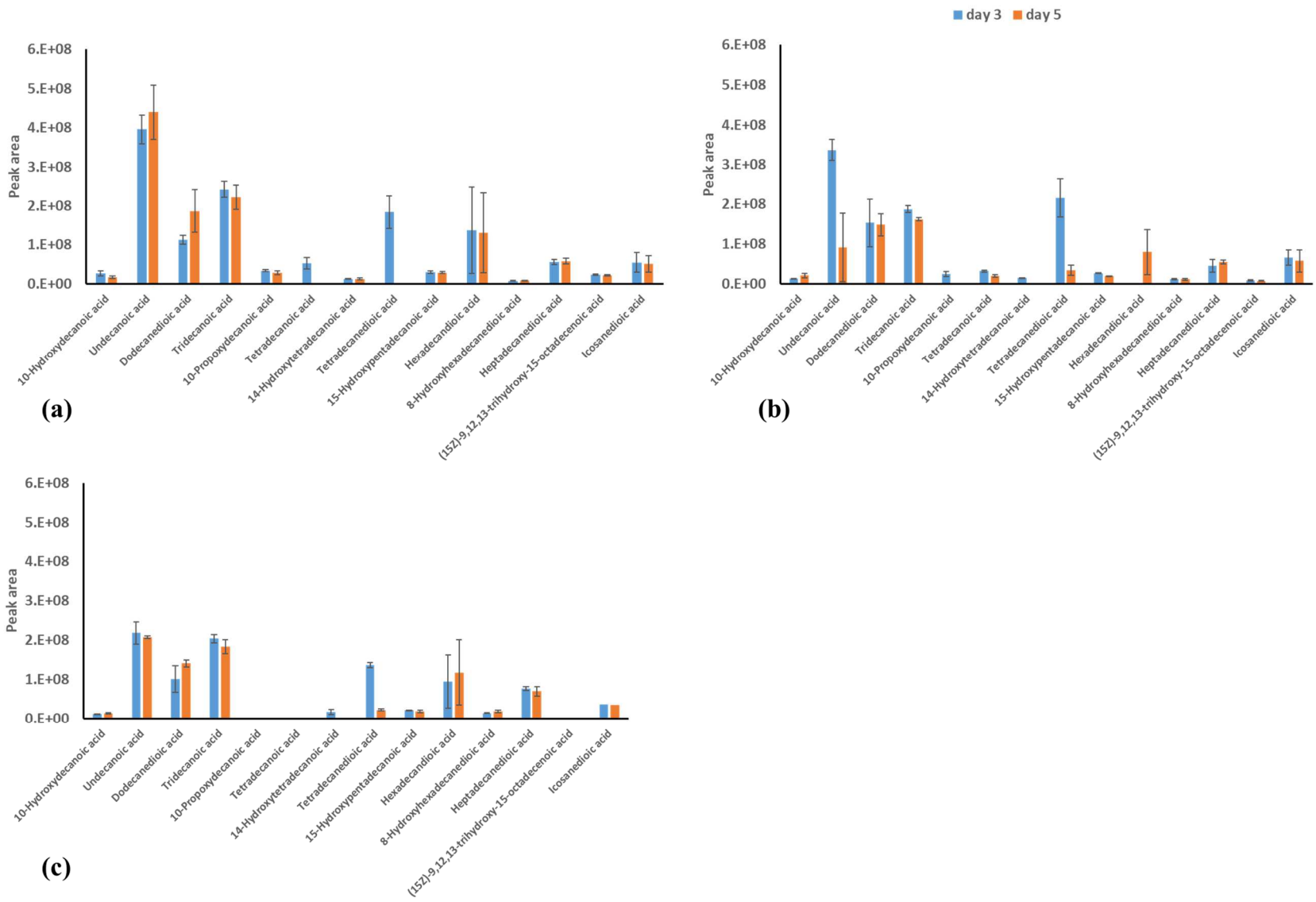
day 3
day 5
Peak area
6.E+08
5.E+08
4.E+08
3.E+08
2.E+08
1.E+08
0.E+00
10-Hydroxydecanoic acid
Undecanoic acid
Dodecanedioic acid
Tridecanoic acid
10-Propoxydecanoic acid
Tetradecanoic acid
14-Hydroxytetradecanoic acid
Tetradecanedioic acid
15-Hydroxypentadecanoic acid
Hexadecandioic acid
8-Hydroxyhexadecanedioic acid
Heptadecanedioic acid
(15Z)-9,12,13-trihydroxy-15-octadecenoic acid
Icosanedioic acid
(a)
(b)
(c)

Captions

Figure 1: Chromatogram showing the relative changes in the profile of saturate fraction of Congo Bilondo crude oils on (a) day 3 and (b) day 5 of biodegradation study. The degradation rates of long-chain alkanes were relatively higher between *Novosphingobium* sp. S1 and *Gordonia amicalis* S2 than with *Gordonia terrae* S5.

Figure 2: The proposed alkane degradation pathway for the three bacteria strains. The produced monocarboxylic acid either can pass on to the β-oxidation pathway or be channelled into the bi-terminal pathway to form dicarboxylic acid.

Figure 3: Levels of carboxylic acids produced from biodegradation of saturate fraction of Congo Bilondo crude oil for (a) *Novosphingobium* sp. S1 (b) *Gordonia amicalis* S2 and (c) *Gordonia terrae* S5.

Tables

Table 1: Percentage weight of fractions of Congo Bilondo crude oil

Composition of fraction (%/weight)				Recovery (%)
Asphaltene	Maltene			
0.3	99.6			99.9
	Saturates	Aromatics	Resins	
	50.4 ± 1.7	32.8 ± 1.3	14.4 ± 0.8	97.6 ± 1.4

Table 2: Hydrocarbons detected by GC-MS in the saturate fractions of Congo Bilondo crude oil. − signifies “not determined”.

Hydrocarbon	**Retention time (min)**	**Molecular formula**	**Molecular structure**	**Amount (μgL^{-1})**	**Quantification ion (m/z)**
n-Decane	7.14	$C_{10}H_{22}$	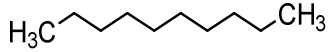	13 ± 1	57
n-Undecane	8.24	$C_{11}H_{24}$	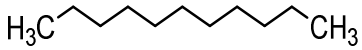	32 ± 8	57
n-Dodecane	9.41	$C_{12}H_{26}$	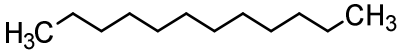	262 ± 46	57
2,3,7 Trimethyloctane	10.29	$C_{11}H_{24}$	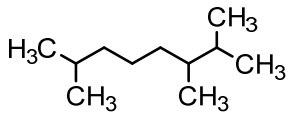	−	−
n-Tridecane	10.62	$C_{13}H_{28}$		105 ± 9	57
4,6-Dimethyldodecane	11.58	$C_{14}H_{30}$	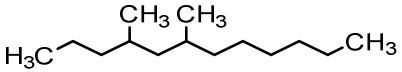	−	−
n-Tetradecane	11.84	$C_{14}H_{30}$	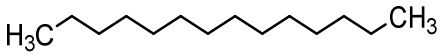	202 ± 18	57
2,6,10-Trimethyltridecane	12.61	$C_{16}H_{34}$	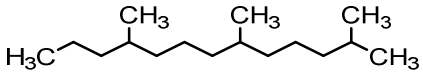	−	−
n-Pentadecane	13.07	$C_{15}H_{32}$	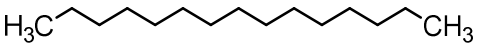	48 ± 2	57
n-Hexadecane	14.26	$C_{16}H_{34}$	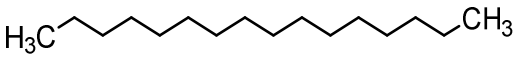	338 ± 68	57
2,6,10-Trimethylpentadecane	14.82	$C_{18}H_{38}$	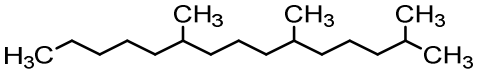	−	−
n-Heptadecane	15.41	$C_{17}H_{36}$		42 ± 3	57
Pristane	15.48	$C_{19}H_{40}$	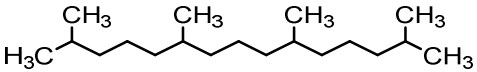	−	−
6-Cyclohexyldodecane	15.89	$C_{18}H_{36}$	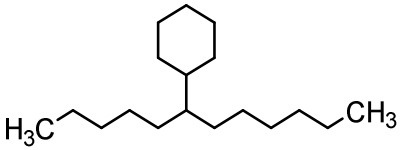	−	−

n-Octadecane	16.51	$C_{18}H_{38}$	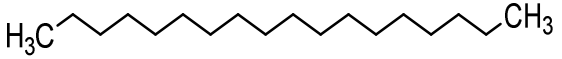	16 ± 4	57
Phytane	16.62	$C_{20}H_{42}$	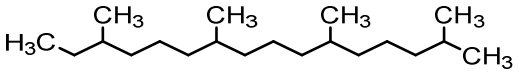	–	–
2-Methyloctadecane	17.42	$C_{19}H_{40}$	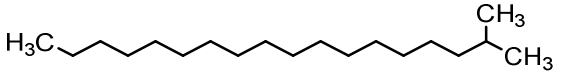	–	–
n-Nonadecane	17.50	$C_{19}H_{40}$	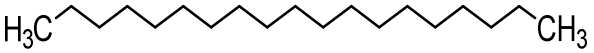	158 ± 41	57
n-Eicosane	18.38	$C_{20}H_{42}$	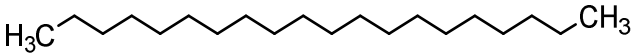	14 ± 3.5	57
n-Heneicosane	19.20	$C_{21}H_{44}$		97 ± 20	57
n-Docosane	19.96	$C_{22}H_{46}$	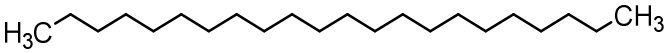	152 ± 29	57
n-Tricosane	20.26	$C_{23}H_{48}$	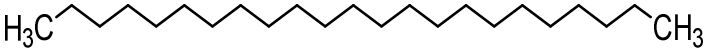	68 ± 3	57
n-Tetracosane	21.77	$C_{24}H_{50}$	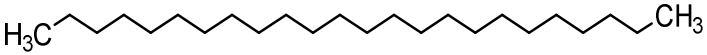	4 ± 1	43
11-methylpentacosane	22.14	$C_{26}H_{54}$	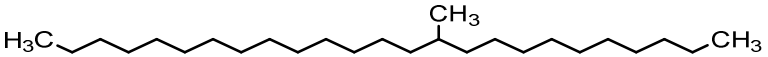	–	–
n-Pentacosane	22.86	$C_{25}H_{52}$		–	–
n-Hexacosane	23.54	$C_{26}H_{54}$	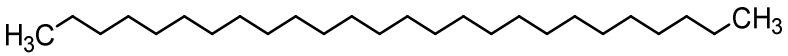	–	–
n-Heptacosane	24.21	$C_{27}H_{56}$	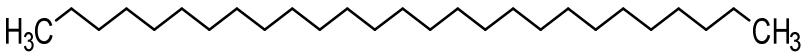	–	–
n-Octacosane	24.75	$C_{28}H_{58}$	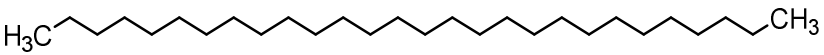	–	–

Table 3: Relative biodegradation efficiency of saturated hydrocarbons on day 3 and 5 of biodegradation study.

	Biodegradation efficiency (%)					
	***Novosphingobium* sp. S1**		***Gordonia amicalis* S2**		***Gordonia terrae* S5**	
Hydrocarbon	**day 3**	**day 5**	**day 3**	**day 5**	**day 3**	**day 5**
n-Decane	64 ± 10	72 ± 9	79 ± 9	81 ± 3	61 ± 8	76 ± 19
n-Undecane	68 ± 1	75 ± 12	64 ± 3	81 ± 15	59 ± 17	86 ± 13
n-Dodecane	76 ± 22	87 ± 13	70 ± 22	81 ± 15	79 ± 16	87 ± 13
2,3,7 Trimethyloctane	94 ± 10	100	95 ± 6	100	100	100
n-Tridecane	45 ± 13	76 ± 22	62 ± 18	81 ± 6	61 ± 10	83 ± 16
4,6-Dimethyldodecane	80 ± 2	84 ± 16	91 ± 1	92 ± 8	79 ± 4	80 ± 3
n-Tetradecane	67 ± 5	78 ± 11	63 ± 15	83 ± 2	71 ± 7	80 ± 3
2,6,10-Trimethyltridecane	100	100	96 ± 4	100	97 ± 3	100
n-Pentadecane	100	100	88 ± 11	100	79 ± 18	100
n-Hexadecane	50 ± 17	75 ± 10	62 ± 25	69 ± 10	47 ± 17	59 ± 12
2,6,10-Trimethylpentadecane	100	100	100	100	94 ± 11	100
n-Heptadecane	100	100	100	100	100	100
Pristane	77 ± 15	87 ± 7	83 ± 11	91 ± 4	72 ± 16	77 ± 5
6-Cyclohexyldodecane	30 ± 4	64 ± 1	52 ± 12	66 ± 1	8 ± 2	26 ± 4
n-Octadecane	81 ± 17	82 ± 16	70 ± 18	85 ± 5	68 ± 9	75 ± 22
Phytane	73 ± 23	100	89 ± 6	98 ± 2	54 ± 3	62 ± 7
2-Methyloctadecane	86 ± 24	87 ± 11	84 ± 9	99 ± 3	67 ± 7	69 ± 4

n-Nonadecane	100	100	100	100	100	100
n-Eicosane	62 ± 12	67 ± 28	73 ± 2	80 ± 5	61 ± 1	66 ± 5
n-Heneicosane	77 ± 3	80 ± 2	65 ± 3	73 ± 7	58 ± 6	60 ± 8
n-Docosane	58 ± 18	72 ± 25	76 ± 13	81 ± 17	58 ± 25	59 ± 6
n-Tricosane	56 ± 1	72 ± 24	71 ± 6	79 ± 20	58 ± 6	62 ± 6
n-Tetracosane	65 ± 14	74 ± 23	72 ± 17	78 ± 20	56 ± 14	56 ± 10
n-Pentacosane	37 ± 4	60 ± 8	62 ± 2	79 ± 4	33 ± 6	34 ± 1
n-Hexacosane	36 ± 9	68 ± 28	65 ± 8	87 ± 6	28 ± 4	42 ± 8
n-Heptacosane	41 ± 8	80 ± 17	71 ± 25	73 ± 29	31 ± 6	46 ± 4
n-Octacosane	32 ± 10	70 ± 26	56 ± 13	72 ± 25	44 ± 5	55 ± 19

Table 4: Carboxylic acids produced from biodegradation of saturate fraction of Congo Bilondo crude oil. ND denotes “Not Detected” and − signifies “Unknown”.

Compound	Molecular formular	Molecular mass	RT	Day detected in culture			Probable precursor
				Novo. sp. S1	*G. amicalis* S2	*G. terrae* S5	
10-Hydroxydecanoic acid	$C_{10}H_{20}O_3$	188.14	6.45	3 and 5	3 and 5	3 and 5	*n*-Decane
Undecanoic acid	$C_{11}H_{22}O_2$	186.16	12.44	3 and 5	3 and 5	3 and 5	*n*-Undecane
Dodecanedioic acid	$C_{12}H_{22}O_4$	230.15	6.37	3 and 5	3 and 5	3 and 5	*n*-Dodecane
Tridecanoic acid	$C_{13}H_{26}O_2$	214.19	13.83	3 and 5	3 and 5	3 and 5	*n*-Tridecane
10-Propoxydecanoic acid	$C_{13}H_{26}O_3$	230.18	10.62	ND	3	3 and 5	−
Tetradecanoic acid	$C_{14}H_{28}O_2$	228.20	15.01	3	3 and 5	3	*n*-Tetradecane
14-Hydroxytetradecanoic acid	$C_{14}H_{28}O_3$	244.20	11.63	3	3	3 and 5	*n*-Tetradecane
Tetradecanedioic acid	$C_{14}H_{26}O_4$	258.18	9.40	3 and 5	3 and 5	3	*n*-Tetradecane
15-Hydroxypentadecanoic acid	$C_{15}H_{30}O_3$	258.21	12.36	3 and 5	3 and 5	3 and 5	*n*-Pentadecane
Hexadecandioic acid	$C_{16}H_{30}O_4$	286.21	11.37	3 and 5	5	3 and 5	*n*-Hexadecane
8-Hydroxyhexadecanedioic acid	$C_{16}H_{30}O_5$	302.20	7.50	3 and 5	3 and 5	3 and 5	*n*-Hexadecane
Heptadecanedioic acid	$C_{17}H_{32}O_4$	300.23	11.99	3 and 5	3 and 5	3 and 5	*n*-Heptadecane
(15*Z*)-9,12,13-trihydroxy-15-octadecenoic acid	$C_{18}H_{34}O_5$	330.24	9.52	ND	3 and 5	3 and 5	−

Icosanedioic acid	$C_{20}H_{38}O_4$	342.27	13.76	3 and 5	3 and 5	3 and 5	*n*-Icosane

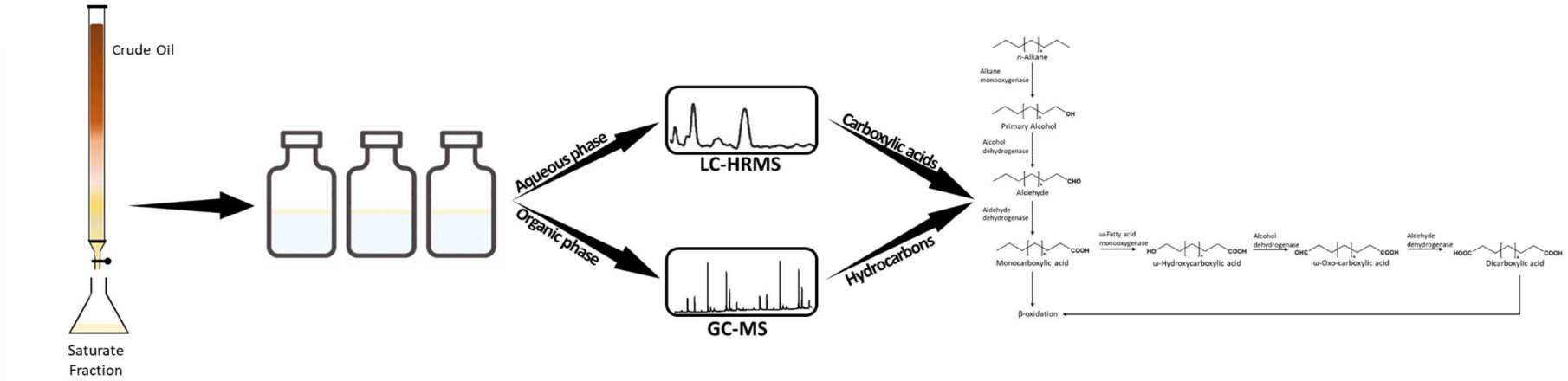

1 SARA Fractionation

2 Aerobic Biodegradation

3 Parallel Analytical Method

4 Metabolic Pathway Reconstruction